Soils and Foundations 2014;54(2):141–154

The Japanese Geotechnical Society

Soils and Foundations

www.sciencedirect.com
journal homepage: www.elsevier.com/locate/sandf

Design approach to a method for reinforcing existing caisson foundations using steel pipe sheet piles

Koichi Isobe[a,*], Makoto Kimura[b], Satoru Ohtsuka[a]

[a]Department of Civil and Environmental Engineering, Nagaoka University of Technology, Nagaoka, Japan
[b]Department of Civil and Earth Resources Engineering, Kyoto University, Japan

The manuscript was received on August 30, 2011 for publication in the Special Issue on "IS-Kanazawa 9th International Conference on Testing and Design Methods for Deep Foundations" published in Vol. 52 No. 6; received in revised form 5 August 2012; accepted 16 November 2013
Available online 13 March 2014

Abstract

This paper proposes a steel pipe sheet pile (SPSP) reinforcement method for existing caisson foundations in water. The technique involves driving SPSPs around the caisson foundation and connecting them to it with reinforcing footing. To support the rational design of reinforcements using this method, the following factors influencing the technique's effectiveness and related mechanical behavior should be considered: (1) the conditions of the caisson/SPSP reinforcement footing connection; (2) the caisson/SPSP flexural rigidity ratio; (3) the distance between the caisson and the SPSP wall; and (4) the pile length. However, as the influence of these factors on the reinforcement effect and mechanical behavior has not yet been clarified, the current method has no standardization for the concept of the load transfer mechanism in reinforced foundation systems, and the ultimate lateral bearing capacity of existing caissons has been largely ignored in previous construction. This paper describes centrifuge model tests and three-dimensional elasto-plastic finite element total stress analysis conducted in relation to real cases in order to identify a more effective and rational reinforcement structure. The static lateral bearing capacity and seismic performance of reinforced foundations were investigated, and the following factors were considered: (1) the conditions of the caisson/SPSP reinforcement footing connection; (2) the caisson/SPSP flexural rigidity ratio; and (3) the pile length. Finally, a structural design flow is proposed based on the experimental and numerical simulation results. A chart to facilitate determination of appropriate reinforcement structures is also presented.

Keywords: Caisson; Bearing capacity; Centrifuge model test; Finite element method; Reinforcement; Steel pipe sheet pile foundation; IGC: E04/H01

1. Introduction

After the Southern Hyogo Prefecture Earthquake of 1995, highway/railway bridge design codes were revised to provide much higher levels of structural safety and reliability against tremors. Seismic reinforcement has been promoted for piers of regular and elevated bridges designed according to the pre-quake code, and most elevated bridges on Shinkansen lines and highways have now been reinforced. However, some river bridges on national and prefectural roads have undergone only limited strengthening. To improve the situation and provide higher reliability for such structures, a project to promote the reinforcement of regular and elevated bridges was implemented from 2004 through 2007. However, when seismic waves hit bridges for which only pier reinforcement has been implemented, relatively weak parts such as foundations may

*Corresponding author.
E-mail address: kisobe@vos.nagaokaut.ac.jp (K. Isobe).
Peer review under responsibility of The Japanese Geotechnical Society.

Production and hosting by Elsevier

http://dx.doi.org/10.1016/j.sandf.2014.02.006

yield because the dynamic characteristics of the entire bridge structure have changed. In this context, it is important for the whole bridge structure, including its foundations, to have a high level of seismic resistance. However, few foundations in Japan have been reinforced due to factors such as the long construction period and high cost involved because of limitations in terms of space and traffic, and the reinforcing effect and mechanism of such strengthening have not been fully investigated. Reinforcement is also required for bridge foundations with insufficient bearing capacity due to liquefaction, riverbed degradation and localized scouring.

The two reinforcement methods recently developed for foundations involve (a) ground improvement and (b) addition of new structures (Japan Road Association, 2000). Both techniques have several possible approaches depending on the reinforcement material used, and their scope of application is limited (Kishishita et al., 2003; Fukada et al., 2005; Nishioka et al., 2008; Bao, X. et al., 2012, etc.). An appropriate method needs to be selected in line with the reinforcement target and ground/construction conditions. Although most of these approaches have already been applied in the field, their reinforcement effects and mechanisms remain unclear, and no specific construction or design methods have been authorized. Accordingly, it is necessary to develop a rational and simple reinforcement method by which the earthquake-proof performance of entire bridge structures can be guaranteed, and to establish techniques for evaluating reinforcement effects, assessing the bearing capacity and seismic stability of existing foundations, and clarifying the required level of seismic stability.

2. Characteristics of the steel pipe sheet pile reinforcement method

This paper outlines the steel pipe sheet pile (SPSP) reinforcement method (Fig. 1), in which SPSPs are installed around existing caisson foundations and their joints are interlocked, and the piles and caisson are connected with a reinforcing footing. The technique increases the lateral bearing capacity of reinforced foundation systems, and is suitable for structures in water because SPSP walls can stop water from entering the work space based on their welded interlocking joint structure (Fig. 2). However, the following factors still need to be clarified for design and construction using the SPSP reinforcement method: (1) the load distribution between the existing caisson and the added SPSP wall; (2) an appropriate footing connection type; and (3) the point bearing capacity of SPSPs installed with limited overhead clearance. Accordingly, the current method has no standardization for the concept of the load transfer mechanism for reinforced foundation systems, and the ultimate lateral bearing capacity of existing caissons

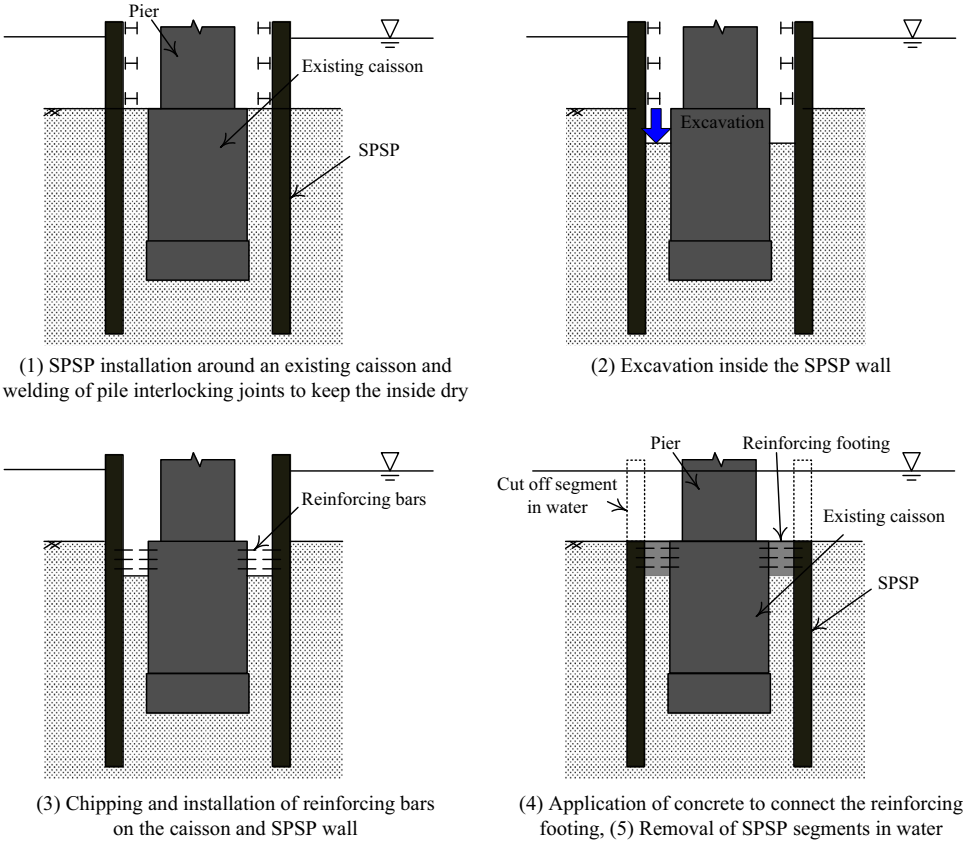

Fig. 1. Construction flow of the SPSP reinforcement method. (1) SPSP installation around an existing caisson and welding of pile interlocking joints to keep the inside dry; (2) excavation inside the SPSP wall; (3) chipping and installation of reinforcing bars on the caisson and SPSP wall; (4) application of concrete to connect the reinforcing footing; and (5) removal of SPSP segments in water.

has been largely ignored in previous construction. As a result, the costs of applying the method tend to be high. This paper proposes more rational and economical SPSP reinforcement approaches, such as simplifying footing connections and reducing the length of SPSPs, to address these considerations.

For rational design and incorporation of these proposals into the SPSP reinforcement method, the following factors influencing the effectiveness of such reinforcements and their mechanical behavior need to be considered: (a) the conditions of the caisson/SPSP wall connection, (b) SPSP length, (c) the caisson/SPSP wall flexural rigidity ratio, (d) the spacing between the caisson and the SPSP wall, and (e) the ground conditions (Fig. 3).

To clarify a more effective and rational reinforcement structure, this paper briefly summarizes the results of centrifuge model tests (Isobe and Kimura, 2005; Isobe et al., 2006), then describes three-dimensional elasto-plastic finite element total stress analysis conducted in relation to real cases. The conditions of the caisson/SPSP wall footing connection and the pile length were considered in the simulation. Finally, a structural design flow is proposed based on the experimental and numerical simulation results. A chart to facilitate determination of appropriate reinforcement structures is also presented.

3. Centrifugal model tests on an SPSP-reinforced caisson foundation

3.1. Outline of centrifuge model tests

Fig. 4 shows the experimental apparatus and model foundation developed by Isobe et al. (2005, 2006). In this setup, a static weight of 200 N was first applied to a steel pier fixed to the foundation system of an SPSP-reinforced model caisson embedded in sandy ground to represent the dead load of the superstructure, and lateral loading at a centrifugal acceleration of 50 G was then applied to the pier. Dry Toyoura sand with a relative density of 90.0% was used as the layer penetrated by the pile. A steel block (Young's modulus: 2.0E08 kN/m^2; Poisson's ratio: 0.29) and a stabilized lime block (Young's modulus: 2.6E06 kN/m^2; Poisson's ratio: 0.25) were used as bearing layer types. Table 1 shows the properties of the model foundation used in the tests, and Fig. 5 shows a cross section of the structure.

In this research, 20 model test cases were conducted as listed in Table 2. Those involving only the caisson were designated as Case-1 tests, which were subdivided into S, M and L types according to the stiffness of the caisson. Those involving the SPSP-reinforced caisson were designated as Case-2 tests, which were subdivided into Type A, Type B and Type C depending on the conditions of the connection between the caisson and the SPSP reinforcement. The terms

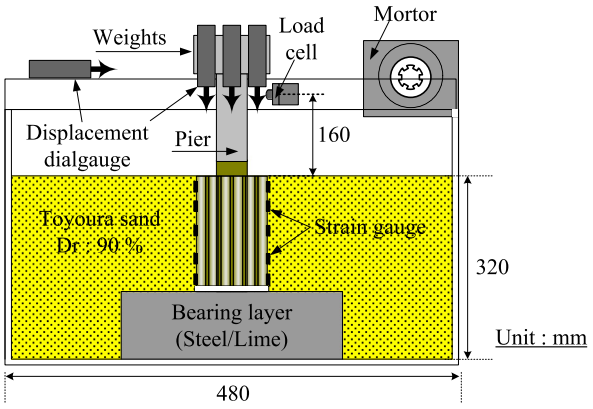

Fig. 4. Cross section of the model test chamber.

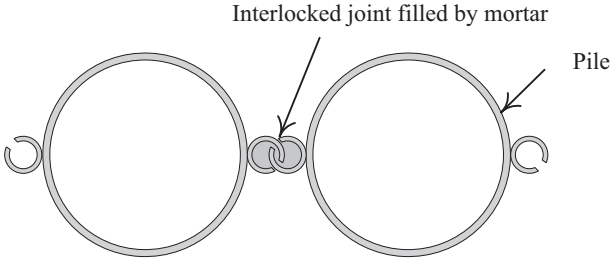

Fig. 2. Cross section of steel pipe sheet piles (SPSPs).

Table 1
Centrifugal test model properties.

SPSP		Caisson			
		Type	S	M	L
Diameter D_p	15 mm	Diameter D_c	50 mm		
Length L_p	200 mm	Length L_c	225 mm		
Thickness t_p	1 mm	Thickness t_c	1 mm	5 mm	Solid
No. of pile	20	Flexural rigidity ratio	0.47	1.33	2.00

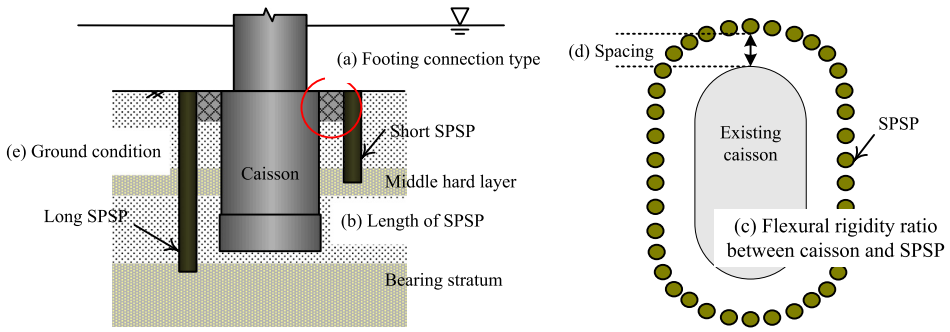

Fig. 3. Design parameters for the SPSP reinforcement method.

Type A, Type B and Type C refer to rigidly fixed, just-touching and free caisson/SPSP connection conditions, respectively, as shown in Fig. 6. In the case of Type B, the SPSP load ratio was measured using a load cell set between the caisson and the SPSP wall. The other details of the experiments are described in Isobe et al. (2006).

4. Experimental results

The influence of caisson/SPSP connection conditions and the flexural rigidity ratio are explained here by comparing the cases shown in Table 2 with the experimental results converted to a prototype scale. Displacement is normalized in relation to the caisson diameter. Figs. 7 and 8 show the lateral load/displacement relationship and the effect of SPSP reinforcement

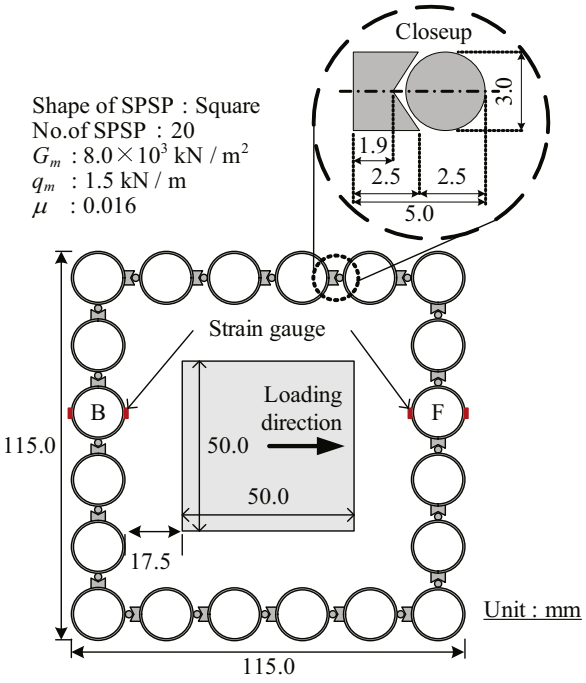

Fig. 5. Cross section of the model foundation.

in cases $2AL_L$, $2BL_L$, $2CL_L$, $2AS_L$, $2BS_L$ and $2CS_L$. This effect is defined as the bearing capacity in Case 2 divided by the bearing capacity in Case 1 for the same displacement. The figures show that the effects of SPSP reinforcement in Cases $2AL_L$ and $2AS_L$ were bigger than 2.5 for displacement values of 5.0%D_c and below. In Cases $2BL_L$ and $2BS_L$, the same tendency as those found in Cases $2AL_L$ and $2AS_L$ was seen. However, the reinforcing effect at 5.0%D_c was 1.3. In Cases $2CL_L$ and $2CS_L$, there was no effect from SPSP reinforcement. Meanwhile, no differences in S and L for Types B and C were observed, but S was bigger than L in Type A.

Fig. 9 shows the applied lateral load/rotation angle relationship and the rotation angle for each case compared at a lateral load of 3.0 MN – the load at which the rotation angle for Cases $1L_L$ and $1S_L$ increased rapidly. It can be seen that the rotation angles of Types A and B were low at approximately 50% of that seen with the caisson only. However, the rotation angle of Type C was almost the same as those seen in Cases $1L_L$ and $1S_L$.

Fig. 10 shows moment distribution on the caisson for each case compared at 3.0 MN. It can be seen that the moments of Cases $2AS_L$ and $2BS_L$ were lower than that of Case $1S_L$ at approximately 50% of that seen with the caisson only. However, the value in Case $2CS_L$ was almost the same as that of Case $1S_L$. Additionally, in the relationship between the rotation angle and the moment distribution on the caisson, the SPSP reinforcement effect is ranked in order of the footing connection degree.

The SPSP load ratio is defined as the total load transmitted from the caisson to the SPSP reinforcement wall (as measured using inner load cells) divided by the total load acting on the SPSP reinforced caisson system. Fig. 11 shows the SPSP load ratio/displacement relationship. The SPSP load ratio for Case $2BL_L$ was constant at 40%, while the value in Case 2BSL increased with displacement from 20% to 60%. This indicates that the ratio is not independent of the caisson/SPSP wall flexural rigidity ratio. Although the former ratio was not ascertained in the other cases due to the difficulty of modeling, the SPSP load ratio is expected to depend on the footing connection type.

Table 2
Centrifugal model test details.

		Caisson (Case-1)	Reinforced caisson system (Case-2)		
			Type-A	Type-B	Type-C
Caisson stiffness	Bearing layer				
 S	Steel	Case-1S_S	Case-2AS_S	Case-2BS_S	Case-2CS_S
	Lime	Case-1S_L	Case-2AS_L	Case-2BS_L	Case-2CS_L
 M	Steel	Case-1M_S	Case-2AM_S	Case-2BM_S	Case-2CM_S
	Lime	–	–	–	–
 L	Steel	Case-1L_S	Case-2AL_S	Case-2BL_S	Case-2CL_S
	Lime	Case-1L_L	Case-2AL_L	Case-2BL_L	Case-2CL_L

Discuss in the present paper

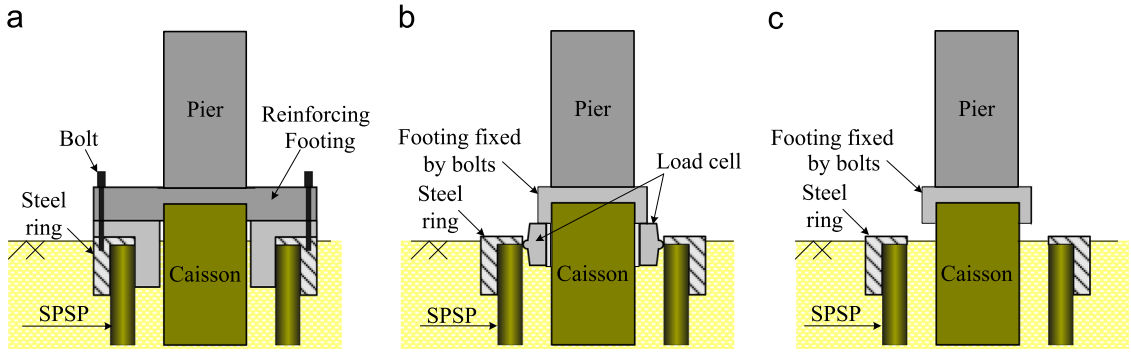

Fig. 6. Cross sections of the three footing connection models. (a) Type-A; (b) Type-B; and (b) Type-C.

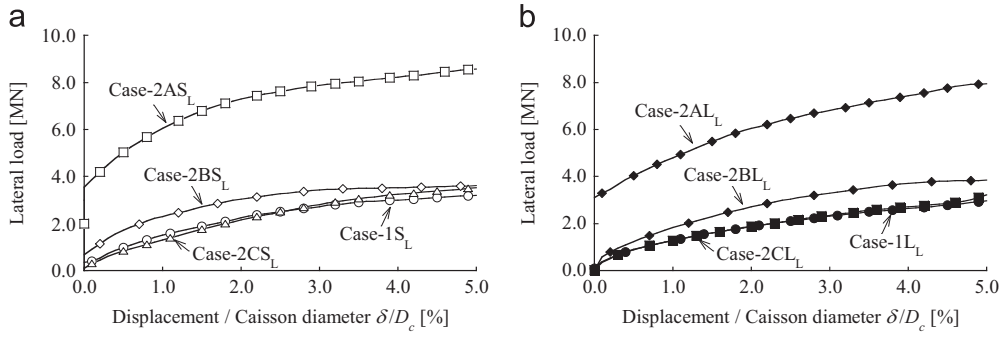

Fig. 7. Lateral load/displacement relationship. (a) S/caisson and (b) L/caisson.

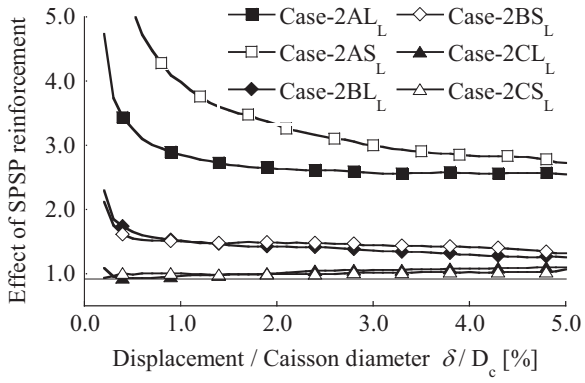

Fig. 8. Effects of SPSP reinforcement.

4.1. Summary

A number of conclusions can be drawn from the results of this experiment. The construction of footing for the SPSP-reinforced caisson to transmit loads from the caisson to the SPSP wall directly is proposed to effectively increase the lateral bearing capacity of the foundation system. However, it may not be necessary to use a rigidly fixed footing (such as that seen with Type A), as a simple Type-B footing connection may suffice. When the flexural rigidity ratio is larger than 1.0, as it was in the case of S, the reinforcement is deemed effective. The load distribution between an existing caisson and an SPSP wall is considered to depend on the flexural rigidity of the caisson in relation to the wall and the degree of bonding for the reinforcement footing.

5. Numerical simulation for the physical mechanism of existing caisson foundations reinforced using the SPSP method

5.1. Purpose of numerical simulation

With the current SPSP reinforcement method, the caisson and SPSPs are connected rigidly via a footing with steel reinforcing bars placed between them. However, the results of the experimental research outlined above show that a simple footing such as sub-slab concrete without reinforcing bars provides the required reinforcement effect. Accordingly, it may not be necessary to apply rigid footing in all cases. In this simulation, the quantitative influence of the footing connection conditions on the effect of SPSP reinforcement and its mechanical behavior was investigated to determine whether a simple condition, such as footing without steel bars (which transfers only lateral loads from the caisson to the SPSP wall) would increase the lateral bearing capacity of the foundation adequately.

5.2. Outline of numerical simulation

The analysis target was an oval-shaped caisson foundation measuring 10.5 m in length, 5.5 m in width and 15.0 m in depth located mainly in sandy soil as shown in Fig. 12 (Isobe

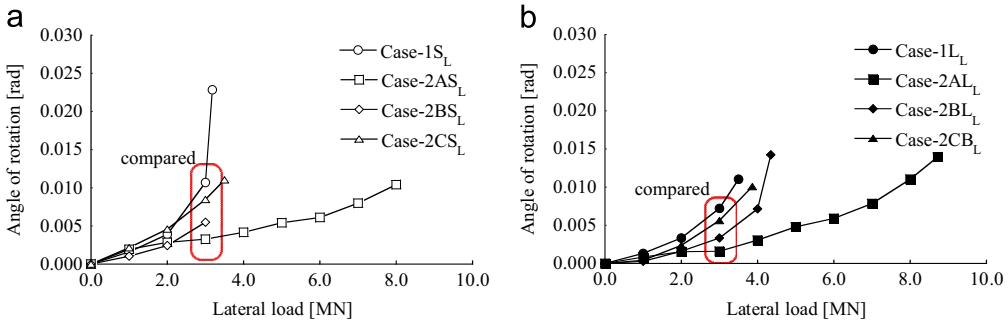

Fig. 9. Lateral load/rotation angle relationship. (a) S/caisson and (b) L/caisson.

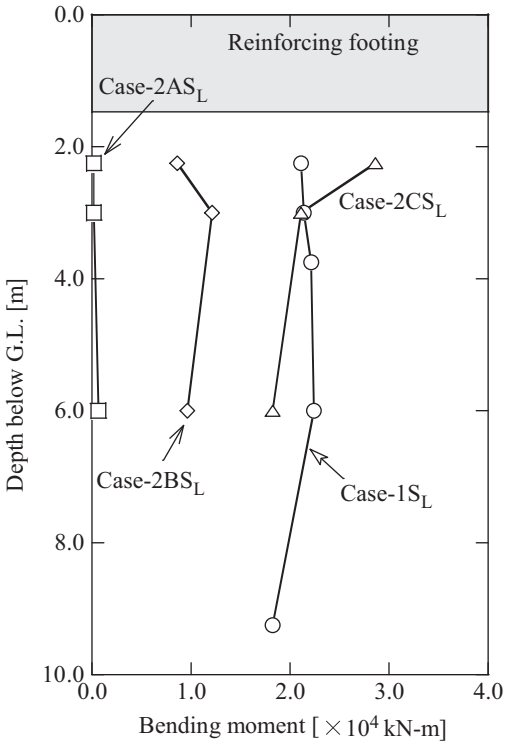

Fig. 10. Caisson moment distribution.

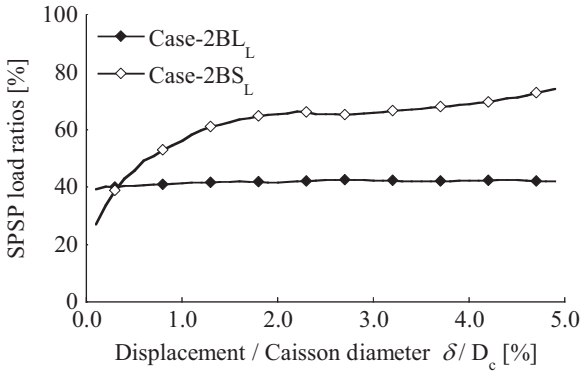

Fig. 11. SPSP load ratio/displacement relationship.

et al., 2007). It was necessary to evaluate the seismic capacity of the caisson due to the occurrence of local scouring around its foundation. The evaluation results showed that the structure would yield and that lateral displacement would increase rapidly against the applicable seismic lateral load because of plastic deformation of the ground in front of the caisson. To increase the lateral bearing capacity of the foundation, the caisson needed to be reinforced using the SPSP method with 38 piles measuring 800 mm in diameter and 15 m in length.

In the simulation, the caisson was simply modeled as a rectangular elastic solid element with a length of 4.0 m, a width of 12.0 m and a depth of 9.0 m in consideration of the effective width of foundations reacting to loads according to Reference for Highway Bridge Design Specifications for Highway Bridges (2002). Young's modulus was set to a value equal to that of the actual flexural rigidity.

The SPSP element was represented using a bilinear beam with three different bilinear springs to model the SPSP joints' vertical shear movement and tangential/normal resistance as shown in Fig. 13(a). The pile volume was not considered in the calculation. The SPSP location was set as the actual distance of 1.5 m from the caisson. Young's modulus was set to a value equal to that of the actual flexural rigidity of the SPSP wall. The nonlinearity of the SPSP piles and springs was calculated according to the relevant design code (2002). The properties of the foundation are also shown in Tables 3 and 4. Fig. 13(b) gives an outline of the footing condition models, which were labeled Type A (fixed type) and Type B (simple type). In the Type-A model, external forces such as lateral loading, vertical loading and moment were transmitted from the caisson to the SPSP wall by the footing. Conversely, in the Type-B model, only lateral loading could be transmitted using the elastic spring element rather than the footing of Type A. The footing was modeled as a sufficiently stiff solid element.

The ground was represented using a Drucker–Prager model modified simply so that when a stress state was on the failure line and the stress increment was judged as loading, adjustment was made to keep the stress state stationary on the failure line (Zhang et al., 2000). This straightforward method keeps the Young's modulus value very low and ensures that plastic strain follows the flow rule. The advantage of the model is its simplicity, in that only four parameters need to be determined, as with the Drucker–Prager model. The parameters of the soil model used in the finite element analysis are shown in Table 5.

In consideration of symmetry and geometrical/loading conditions, only half of the domain was used in the analysis.

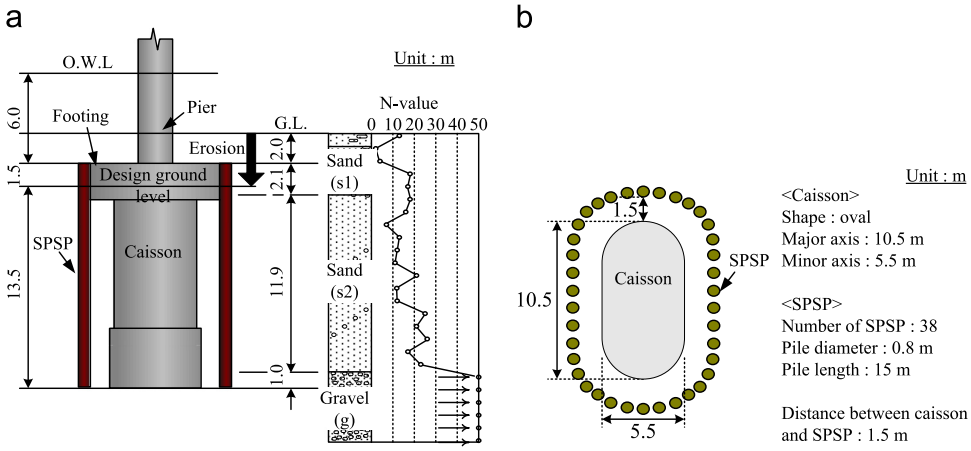

Fig. 12. Analysis target. (a) Analysis example and soil boring log and (b) cross section of foundation.

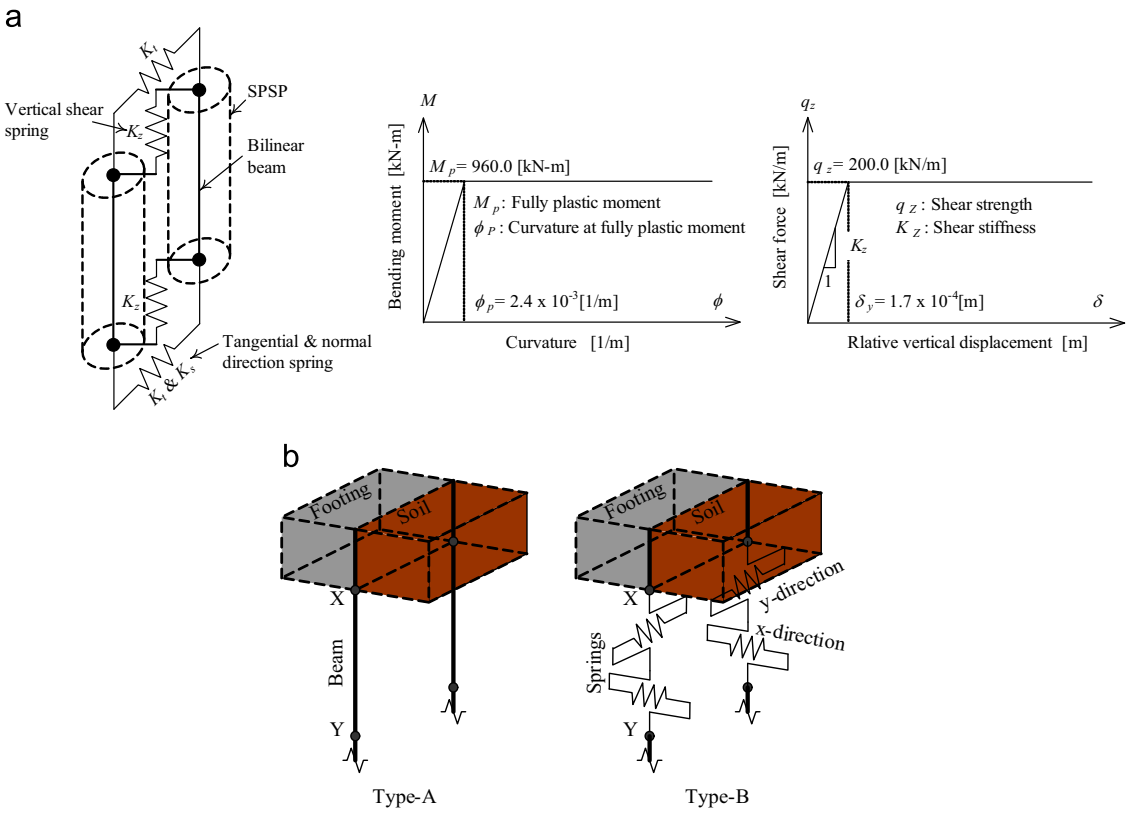

Fig. 13. Modeling used in the simulation. (a) SPSP and (b) footing connection.

Table 3
Simulation caisson model properties.

	Major axis B [m]	Minor axis D [m]	Length L_c [m]	Young's modulus E_c [kN/m^2]	Poisson's ratio ν_c –	Geometric moment of inertia I_c [m^4]	Flexural rigidity EI_c [kN-m^2]
Prototype	10.5	5.5	15.0	2.5×10^7	0.17	99.3	2.5×10^9
Model	9.4	4.4	15.0	3.7×10^7	0.17	66.7	

A finite linear element mesh was prepared as shown in Fig. 14. The boundary conditions were (a) the bottom of the ground was fixed; (b) the vertical boundaries parallel to the XOZ plane were fixed in the y direction and free in the x and z directions; (c) the vertical boundaries parallel to the YOZ plane were fixed in the x direction and free in the y and z directions. These

Table 4
Simulation SPSP model properties.

(a) Piles

	Diameter ϕ [m]	Thickness t [mm]	Length L_p [m]	Yield strength σ_y [MPa]	Yield Moment M_y [kN-m]	Young's modulus E_p [kN/m^2]	Sectional area A [m^2]	Flexural rigidity EI_p [kN-m^2]
Prototype	0.8	9.0	15.0	235.0	960.0	2.0×10^8	0.022	1.6×10^9
Model	0.8	9.0	15.0	235.0	960.0	2.3×10^8	0.022	

(b) Joints

	Shear stiffness K_z [kN/m^2]	Shear strength q_z [kN/m]	Tangential direction stiffness K_t [kN/m^2]	Tangential direction compressive strength q_{tc} [kN/m]	Tangential direction tensile strength q_n [kN/m]
Prototype	1.2×10^6	200	5.0×10^6	5000	280
Model	1.2×10^6	200	5.0×10^6	5000	280

Table 5
Soil properties.

	Thickness H [m]	N-value N –	Density γ [kN/m^3]	Young's modulus E [kN/m^2]	Internal friction angle ϕ [deg]	Cohesion c [kPa]	Poisson's ratio ν –
Sand (s1)	0.6	16	18.0	9.0×10^4	30.0	0.0	0.33
Sand (s2)	11.9	17	18.0	9.5×10^4	30.0	0.0	0.33
Gravel (g)	4.5	50	20.0	2.8×10^5	40.0	0.0	0.33

calculations were conducted under drained conditions, meaning that pore water pressure was not considered.

A prescribed incremental load was applied in one direction, and vertical and lateral loading were divided into 20 and 200 steps, respectively. In Case 3, V (the vertical load) was 20.9 MN, H (the horizontal load) was 9.5 MN, and M (the moment) was 100.5 MN-m. In Case 4, V was 18.4 MN, H was 11.6 MN, and M was 105.2 MN-m. In Case 5, V was 23.4 MN, H was 11.6 MN, M was 105.2 MN-m, and the weight of the footing was added to the vertical load. The required seismic coefficient for L1 and L2 earthquake is 0.3 and 1.0 for each case, respectively. In the simulation, verification was performed to determine whether displacement and the rotation angle were suppressed to below acceptable values against the required level of horizontal resistance; that is, whether they were prevented from increasing rapidly when the required horizontal load was applied. The details of the analysis are shown in Table 6. In the dynamic analysis, a wave from the Southern Hyogo Prefecture Earthquake of 1995 observed at JR West's Takatori Station was used as input, stiffness proportional damping with a damping rate of 5% was applied for the damping model, and the Newmark-β method was used for time integration. To investigate the influence of pile length on SPSP reinforcement effectiveness and the load transfer mechanism, a parametric study on pile length was also conducted. As you know, the strain hysteresis behavior is important in the dynamics analysis. In the present paper, however, the same constitutive model was used in all cases to compare the tendency regarding stiffening effect by SPSP in the dynamic simulation with those in the static analysis. The DGPILE-3D analysis code (Kimura and Zhang, 2000; Zhang and Kimura, 2002), which is important basis for DBLEAVES (Ye et al., 2007; Bao, Y. et al., 2012) was used for the numerical simulation.

5.3. Analysis results and discussion

Figs. 15 and 16 show the relationship between lateral load and displacement for cases 3–5, and that between the reinforcement effect and displacement for case 5. The reinforcement effect is defined as the increase in the ratio of lateral bearing capacity based on the results shown in Fig. 15. Figs. 17 and 18 show the relationship between lateral load and the rotation angle for cases 3–5, and that between the effect of reinforcement on the rotation angle and the lateral load for Case 5. The effect of reinforcement on the rotation angle is defined as the angle suppression effect based on the results shown in Fig. 17. The qualitative nature of the simulation results is the same as that of the experimental results; that is, foundation yielding was seen with rapid increases in the lateral displacement and rotation angle with Type C, but not with Types A and B. It can therefore be inferred that foundation types in which the footing directly

transfers external forces from the caisson to the SPSP wall (i.e., types A and B) have a high reinforcement effect, while that of foundations in which the SPSP wall and caisson are not connected (i.e., Type C) is not sufficient to adequately increase the lateral bearing capacity. Furthermore, greater lateral displacement and rotation angles were observed for small loads with Type C due to constraint of the subgrade reaction area. Besides, the simulation was conducted based on much finer and wider mesh in order to confirm the influence of the mesh size and boundaries to the results regarding lateral displacement, rotation angle and the others. The simulation results of Case-3 and 4 using the finer and wider mesh were shown in Figs. 15 and 17. These figures indicated that their influence was hardly observed in the present simulation case.

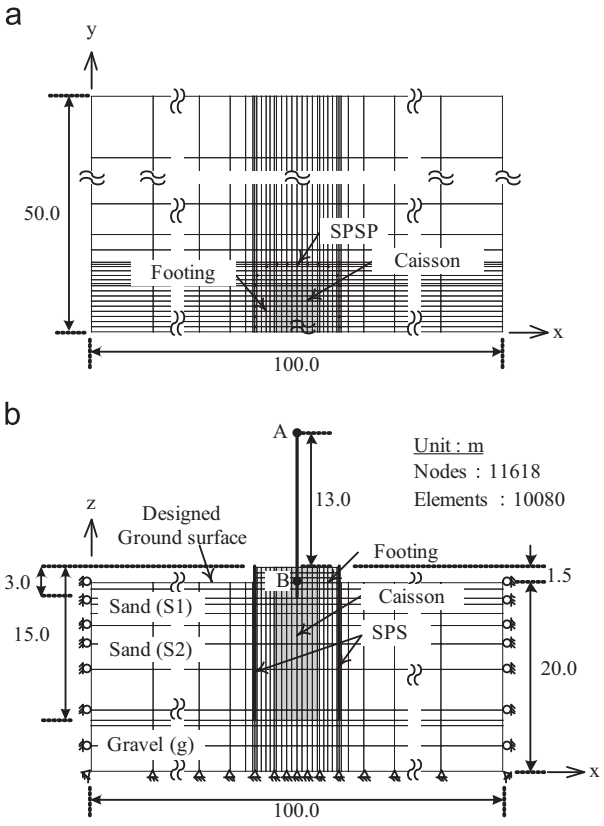

Fig. 14. Front view of the finite element mesh used in the simulation. (a) Plane view and (b) front view.

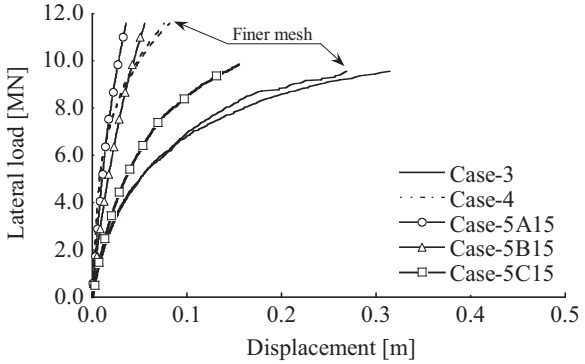

Fig. 15. Relationship between lateral load and displacement for cases 3–5.

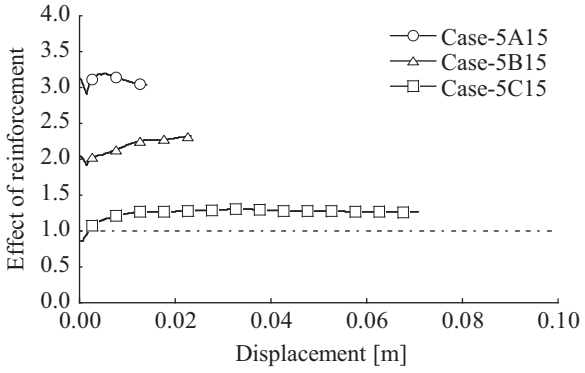

Fig. 16. The reinforcement/displacement curve effect in Case 5.

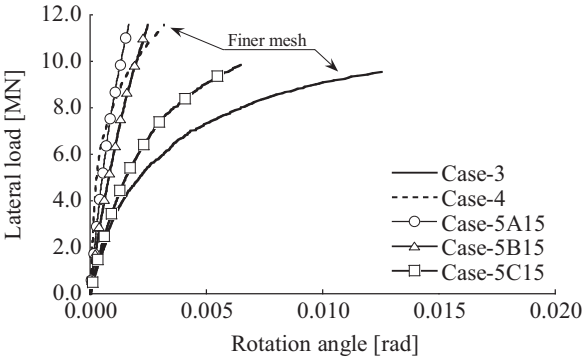

Fig. 17. Relationship between lateral load and rotation angle for cases 3–5.

Table 6
Analysis details.

	Caisson (Case-3)	SPSP wall (Case-4)	Reinforced caisson (Case-5)		
			Fixed	Intermediate	No footing
Sketch					
Analytical case	Case-3	Case-4	Case-5A15 Case-5A10 Case-5A05	Case-5B15 Case-5B10 Case-5B05	Case-5C15 Case-5C10 Case-5C05

The axial force and moment distribution of the piles is shown in Fig. 19, which indicates the results for cases 4, 5A15, 5B15, 5A10 and 5B10. In the axial force results, positive values represent compressive force, and negative ones represent tensile force. The graph details for Cases 4 and 5A15 show that compressive force acted on Pile 19 (located in the front of the caisson against the loading direction), and that tensile force acted on Pile 1 (located behind the caisson in the loading direction). The value for Type A was smaller than that seen in Case 4. Conversely, the axial force is almost zero in the graph for Type B. In the results for the moment acting on piles, Case 5B10 shows the highest value, while those for cases 5A15 and 5A10 are very small. The moment generated on piles in all cases did not surpass the pile yield moment.

Fig. 20 shows pile deformation distribution for each case. Compared with the maximum displacement of the pile head for Case 4, the maximum displacement for cases 5A15, 5B15 and 5C15 was lower because the existing caisson shared external loading with the SPSP wall. Fig. 21 shows the lateral ratio of the load shared by the wall. The x axis represents the lateral load applied, and the y axis represents the lateral load shared by the SPSP wall, which is the total share of force observed in the nodes of the footing bottom. In Case 4, 40% of the lateral load was shared by the SPSP wall until its value reached 5 MN, and the ratio then increased to 50% at loading values under 10 MN. The point at which it increased corresponded to the time when lateral displacement increased. Although the ratio of the load shared by the SPSP wall in cases 5A15 and 5B15 was smaller than that seen in Case 4, the same tendency was observed with values between 30% and 45%. The SPSP load ratio for Case 5A15, in which the footing was rigidly connected between the caisson and the SPSP wall, was smaller than that for Case 5B15. This can be explained by the difference in the load transfer mechanisms. The deformation of the SPSP wall and footing in Section A-A at maximum loading is shown in Fig. 22. In Cases 4 and 5A15, the front pile (Pile 19) penetrated the bearing layer, and the back pile (Pile 1) was pulled out. In Case 5B15, the SPSP wall exhibited swaying with no relation to the displacement and rotation behavior of the footing.

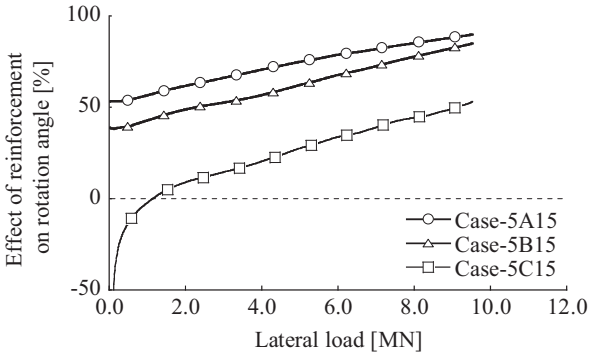

Fig. 18. The reinforcement/displacement curve effect in Case 5.

Fig. 23 shows the relationship between the reinforcement effect and pile length based on the effect at the point of maximum lateral loading. It can be seen that the reinforcement effect of Type A was greater than that of Type B, and a tendency for less effect with shorter piles is observed. The same tendency is also seen in the results for the lateral load/rotation angle relationship. This is especially evident with Type A, and can be explained by differences in SPSP wall deformation as shown in Fig. 22.

Figs. 24 and 25 show dynamic simulation results for factors such as response acceleration, lateral displacement at the head of the foundation and the rotation angle for cases 3 and 5,

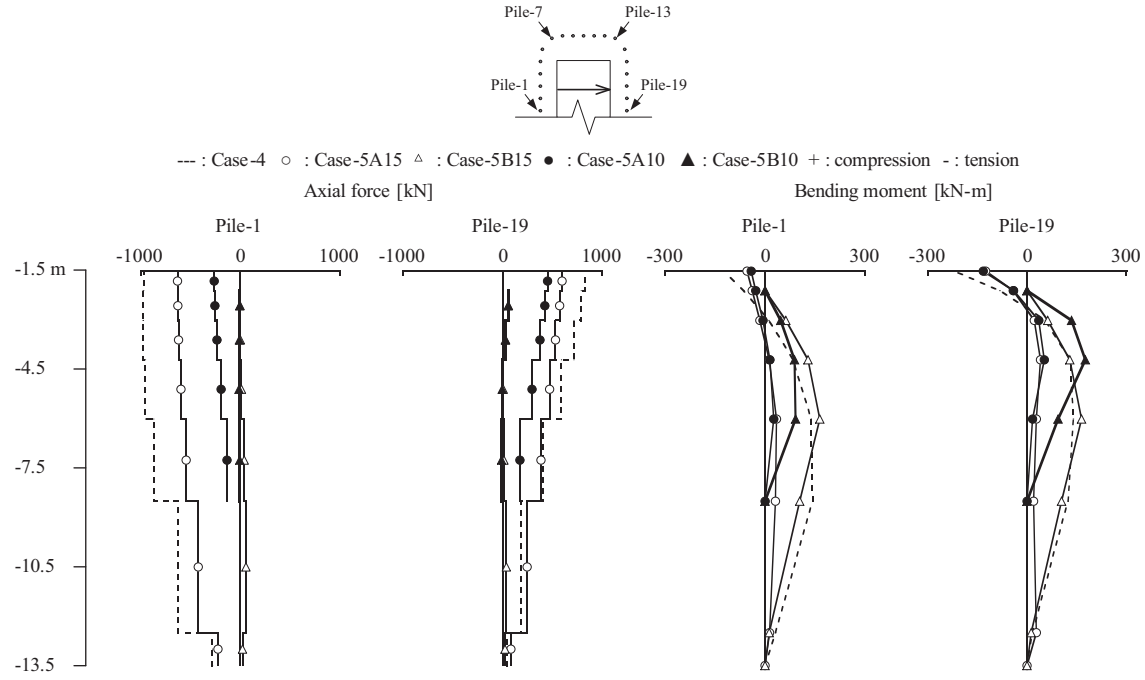

Fig. 19. Axial force and moment distribution on piles at a lateral load of 9500 kN.

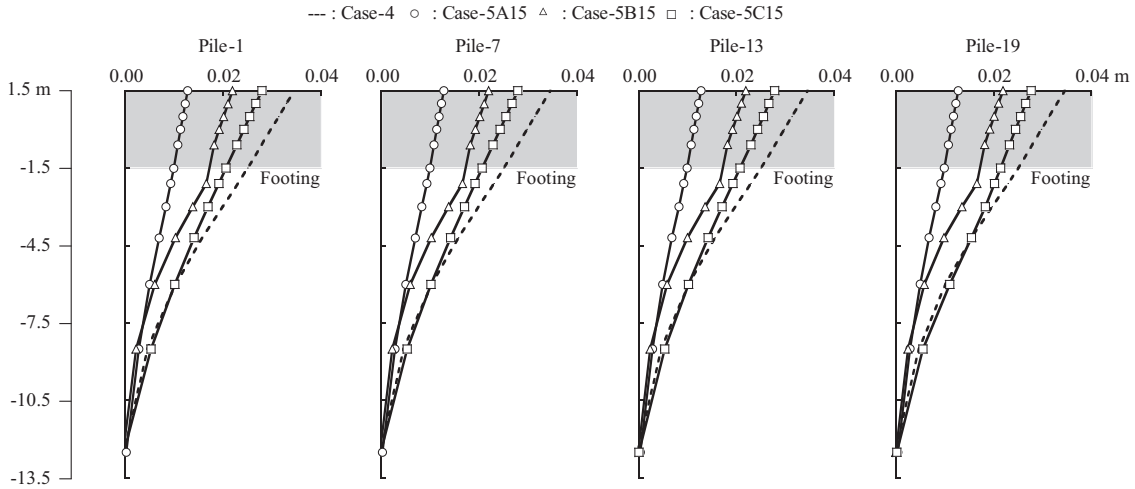

Fig. 20. Pile displacement in the simulation at a lateral load of 9500 kN.

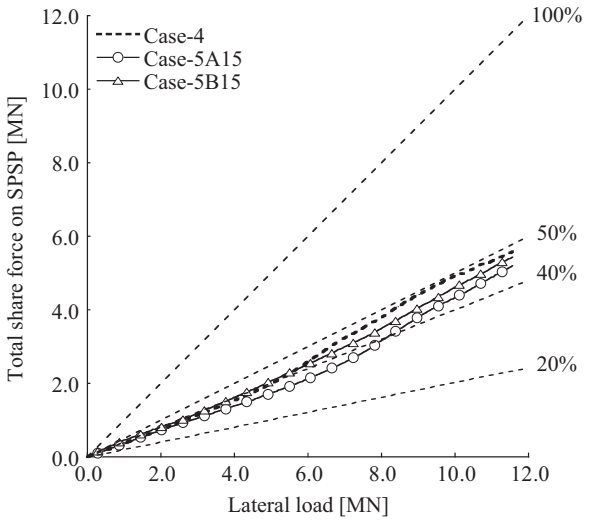

Fig. 21. SPSP load ratio for cases 4 and 5.

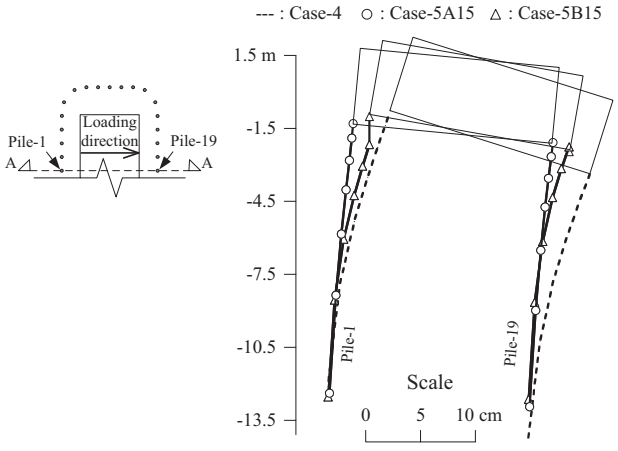

Fig. 22. Deformation of SPSP wall and footing.

respectively. Fig. 26 shows the suppression effect on displacement and the rotation angle at the time when their maximum values were observed for Case 5. In the dynamic simulation

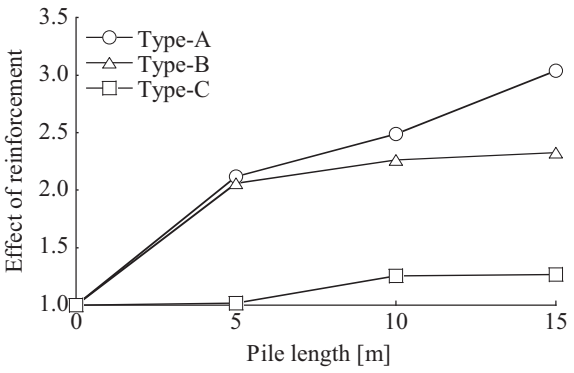

Fig. 23. Relationship between the reinforcement effect and pile length.

results, the same tendency for the footing connection type as those seen in the experiment and the static simulation is observed.

From these results, the following summaries can be made regarding the SPSP reinforcement mechanism of each footing condition:

(1) The caisson and SPSP wall moved together in Type A (the rigidly fixed type). Accordingly, the lateral bearing capacity was higher due to increased subgrade reaction attributable to the larger area of ground resisting the foundation, the bending resistance of the piles, and the end bearing and friction force of the piles. All vertical joints oriented parallel to the loading direction yielded, and the stress of the tangential joints was much smaller than the strength of these joints.

(2) In Type B, the front piles were first loaded laterally with the footing, followed by the side piles and the back piles with joints between them. The lateral bearing capacity was higher due to increased subgrade reaction attributable to the larger area of ground resisting the foundation and the bending resistance of the piles. With this type, as the end bearing and friction force of the piles cannot be considered, the lateral ratio of the load shared by the SPSP wall was

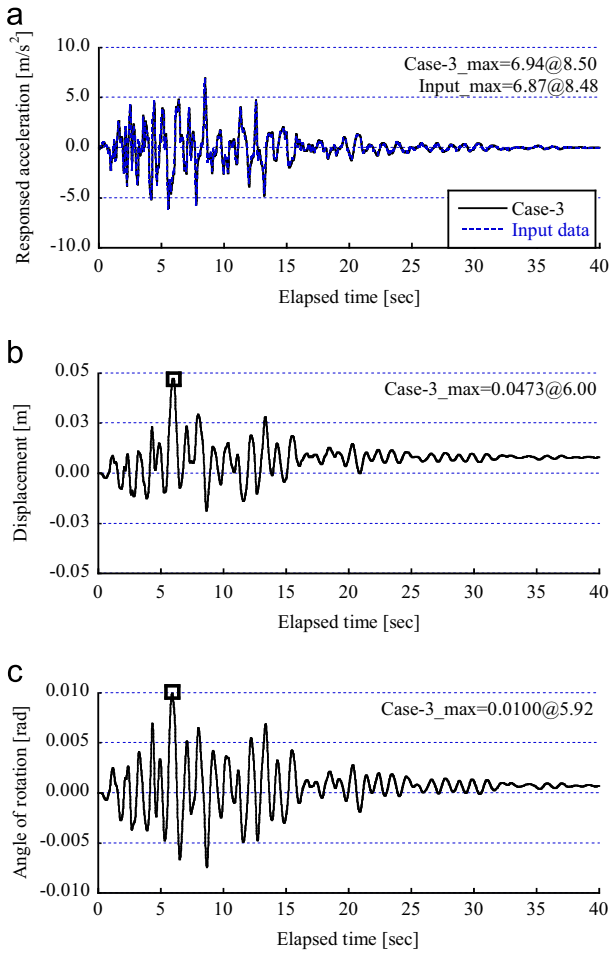

Fig. 24. Response acceleration, lateral displacement of footing top and rotation angle for Case-3. (a) Response acceleration; (b) lateral displacement; and (c) rotation angle.

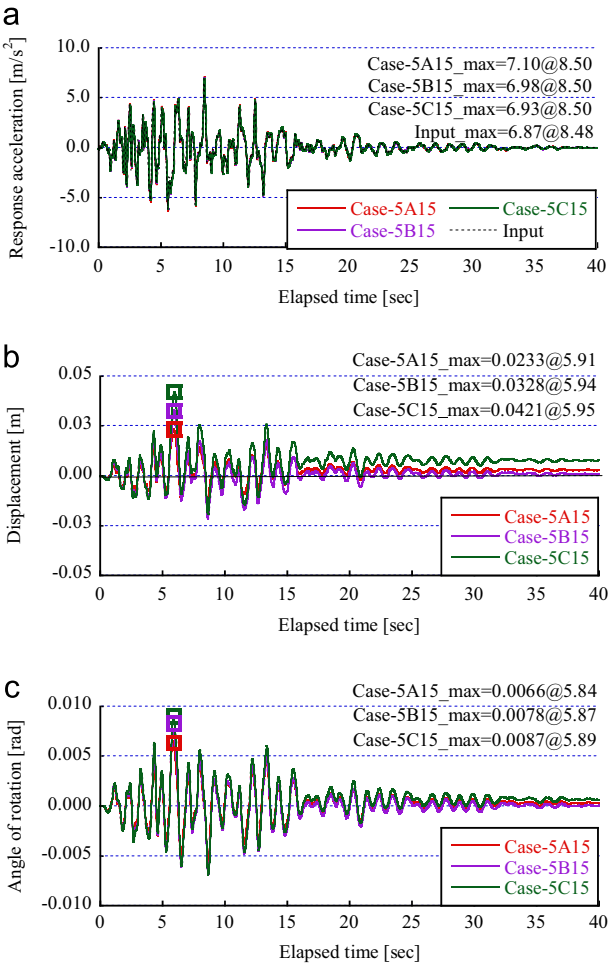

Fig. 25. Response acceleration, lateral displacement of footing top and rotation angle for Case-5. (a) Response acceleration; (b) lateral displacement; and (c) rotation angle.

greater than that for Type A. However, the moment of the piles did not surpass the yield value, and the stress of the vertical and tangential joints did not exceed the strength of these joints.

(3) Shorter piles resulted in a lower SPSP reinforcement effect, and the difference between Type A and Type B became smaller with shorter piles. This is because the friction force of piles in Type A was smaller with shorter piles, and hardly any pile friction force was seen in Type B.

(4) In the dynamic simulation results for the case where pore water pressure was not considered, no significant differences from the static simulation results were observed. Dynamic characteristics in relation to the lateral resistance of SPSP-reinforced foundations have a qualitative nature in common with static characteristics.

6. Proposal of a useful structural selection chart for the SPSP reinforcement method

6.1. Characteristics of the SPSP reinforcement method

A new rational design for the SPSP reinforcement method based on the research outlined above is proposed here. In this

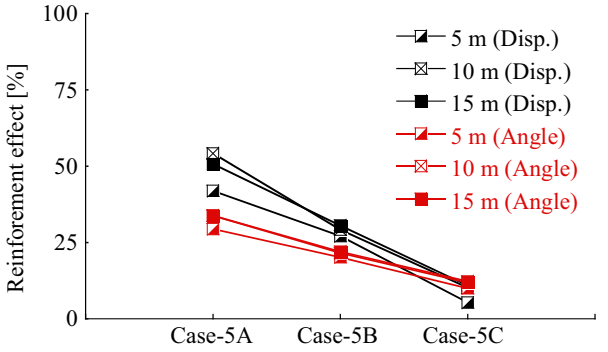

Fig. 26. The suppression effect on displacement and rotation angle for Case-5.

design, the following factors should be appropriately considered so that the reinforced foundation rationally satisfies the required level of seismic capacity: (a) the footing connection type, (b) the SPSP length, (c) the caisson/SPSP flexural rigidity ratio, (d) spacing between the caisson and the SPSP wall, and (e) ground conditions, as shown in Fig. 3. The findings of related centrifuge model tests and numerical simulation results are summarized below.

6.1.1. (a) Footing connection type

The foundation system in which the existing caisson and the SPSP wall were rigidly connected (Type A) had a superior stiffening effect. It was found that the foundation with a simple footing connection type (Type B) may also meet the lateral bearing capacity requirements for reinforced caisson foundations. However, the mechanism behind load transfer from the caisson to the SPSP wall differs significantly between Type A and Type B.

6.1.2. (b) SPSP length

In cases where no vertical bearing capacity increment is necessary or a reinforced foundation with a Type-B footing connection meets the lateral bearing capacity requirements, it is permissible to install the SPSP walls in a middle hard layer.

6.1.3. (c) Caisson/SPSP flexural rigidity ratio

The caisson/SPSP flexural rigidity ratio significantly influences the load share ratio of the existing caisson and the additional SPSP wall for Type B.

6.1.4. (d) Spacing between caisson and SPSP wall

The minimum spacing between the caisson and the SPSP wall should be determined in consideration of the required lateral bearing capacity and appropriate provision of work space.

6.1.5. (e) Ground conditions

The stiffening effect is highly influenced by ground conditions.

The above findings indicate that SPSP-reinforced caisson foundation systems can be more economically and rationally designed based on simplification of the footing connection or reduction of the SPSP length.

6.2. Outline of the proposed design method

Fig. 27 shows a design flow chart. In this design, investigation is first performed to determine whether the stiffness of the existing caisson meets the seismic capacity requirements with the current design method such as the reference (Chioua et al., 2012). If not, calculation of the necessary strength and design of a suitable cross-section structure for the reinforced foundation follow in the flow chart. The required multiplication factor for the stiffness of the reinforced foundation is calculated using an equation that incorporates the design horizontal seismic coefficient of the reinforced foundation and the yield seismic coefficient of the existing foundation as shown in Fig. 28. The cross-section structure is determined in consideration of the shape and size of the existing caisson foundation, the construction method (e.g., SPSP installation) and the work space necessary to connect the footing. Secondly, the connection method and pile length are determined using the structural selection chart shown in Fig. 29. Finally, the seismic capacity of the reinforced foundation system is checked using the three-dimensional frame analysis method developed by Sugano et al. (2009) and Inazumi et al. (2009). In the analysis, all members of the reinforced foundation system and ground resistance are modeled using beams and springs, whose non-linearity creates a bilinear model.

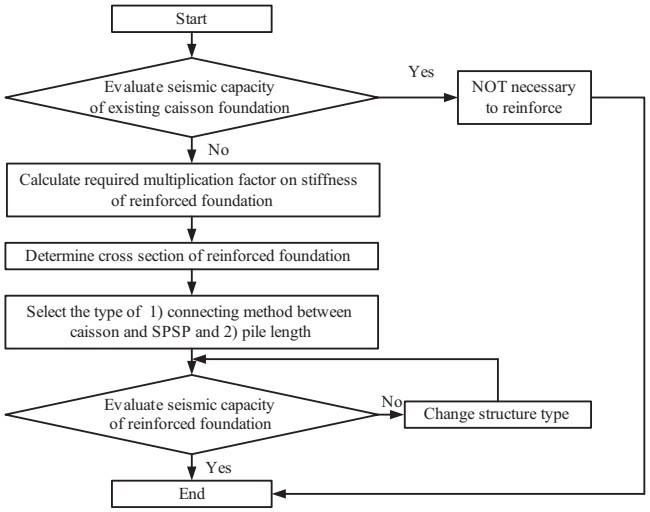

Fig. 27. Design flow of the SPSP reinforcement method for existing caisson foundations.

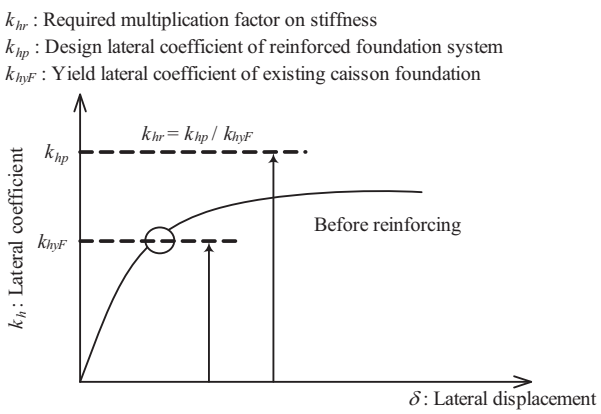

Fig. 28. Definition of the required multiplication factor for reinforced foundation stiffness.

6.3. Outline of the proposed structural selection chart

This section describes the structural selection chart. The x axis represents the SPSP foundation/existing foundation flexural rigidity ratio, and the y axis shows the required multiplication factor. The space is divided into areas I–V according to the footing bonding conditions and pile length based on the results of model tests and FEM analysis (including cases other than those described above). Area I relates to the existing method in which Type A is used for the footing connection and piles are installed in the bearing layer; Area II relates to Type A with piles installed in the middle hard layer (rather than in the bearing layer); Area III relates to Type B with piles installed in the bearing layer; and Area IV relates to Type B with piles installed in the middle hard layer. The chart can be used to establish the footing connecting type and pile length after determination of the reinforced foundation system's cross-section structure and calculation of the required multiplication

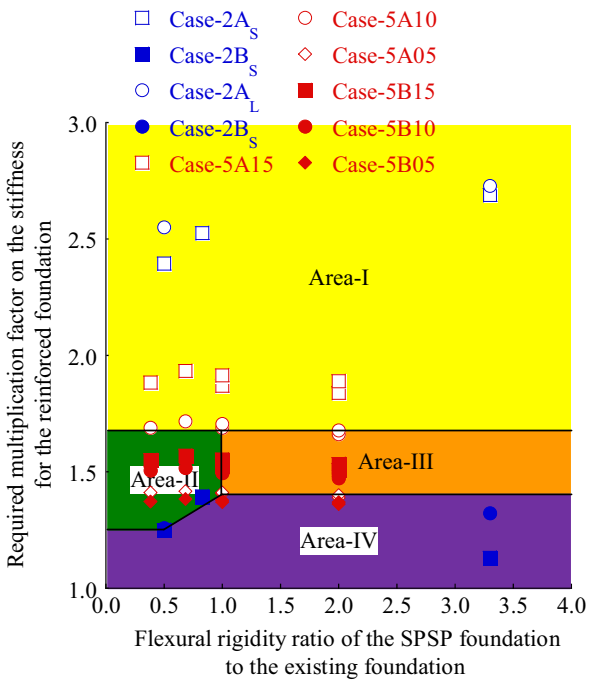

Fig. 29. Proposed structural selection chart for the SPSP reinforcement method (monogram).

factor. The stability of the reinforced foundation structure is checked using the three-dimensional frame analysis method.

7. Conclusions

The main objectives of this research were to develop a rational and economical SPSP reinforcement method in order to solve problems in construction and design, to clarify the effects and mechanism of this method, and to propose rational design for the SPSP reinforcement method. The main conclusions are outlined below.

(1) Construction of reinforcing footing on an SPSP-reinforced caisson to directly transmit loads from the caisson to the SPSP wall can be implemented to effectively increase the lateral bearing capacity of the foundation system. However, it may not be necessary to use rigidly fixed footing; simple footing connection conditions may suffice.
(2) Load distribution between the existing caisson and the SPSP wall depends on the flexural rigidity between the caisson and the wall and the degree of reinforcement footing bonding.
(3) The reinforcement effect is reduced with shorter SPSPs. It is permissible to install SPSP walls in a middle hard layer if necessary.
(4) The minimum spacing between the caisson and the SPSP wall should be determined in consideration of the required lateral bearing capacity and the provision of adequate work space.
(5) These findings support the proposal of a new rational design for the SPSP reinforcement method and a useful structural selection chart along with the 3D frame analysis method.

Acknowledgment

The authors thank the Japanese Association for Steel Pipe Piles for the active discussion and useful information provided in relation to this study. Thanks also go to Messrs. K. Danno (a former graduate student at Kyoto University) and S. Kimura (a former undergraduate student at Nagaoka University of Technology) for their contribution to the experimental and analytical study.

References

Bao, X., Morikawa, Y., Kondo, Y., Nakamura, K., Zhang, F., 2012. Shaking table test on reinforcement effect of partial ground improvement for group-pile foundation and its numerical simulation. Soils Found. 52 (6), 1043–1061.
Bao, Y., Ye, G., Ye, B., Zhang, F., 2012. Seismic evaluation of soil–foundation–superstructure system considering geometry and material nonlinearities of both soils and structures. Soils Found. 52 (2), 257–278.
Chioua, J., Ko, Y., Hsu, S., Tsai, Y., 2012. Testing and analysis of a laterally loaded bridge caisson foundation in gravel. Soils Found. 52 (3), 562–573.
Fukada, H., Kato, K., Aoyagi, M., Ooya, T., Shioi, Y., 2005. A study of reinforcing methods for existing bridges on soft ground with solidification improvement. In: Proceedings of the 50th Symposium on Geotechnical Engineering, pp. 319–326.
Inazumi, S., Isobe, K., Kimura, M., Mitsuda, Y., 2009. Evaluation of mechanical characteristics of joint sections in steel pipe sheet piles and development of 3D-frame structural analysis for the design of SPSP foundations. Doboku Gakkai Ronbunshuu C 65 (2), 532–543 (in Japanese).
Isobe, K., Kimura, M., 2005. Mechanical behavior of caisson foundation reinforced by steel pipe sheet piles. In: Proceedings of the 16th International Conference on Soil Mechanics and Geotechnical Engineering, vol. 4, pp. 1493–1496.
Isobe, K., Kimura, M., Yoshizawa, Y., Kohno, K., Harata, N., Makino, T., 2006. Centrifugal model tests on lateral bearing capacity of existing caisson foundation reinforced by steel pipe sheet piles. Doboku Gakkai Ronbunshuu C 62 (1), 191–200 (in Japanese).
Isobe, K., Kimura, M., Zhang, F., Kohno, K., Harata, N., Makino, T., Kuwajima, T., 2007. Finite element method analysis on mechanical behavior of existing caisson foundation reinforced by steel pipe sheet piles. Doboku Gakkai Ronbunshuu C 63 (2), 516–529 (in Japanese).
Japan Road Association, 2000. Reference for Reinforcement of Existing Highway Bridge Foundations, Japan Road Association.
Kimura, M., Zhang, F., 2000. Seismic evaluations of pile foundations with three different methods based on three-dimensional elastic–plastic finite element analysis. Soils Found. 40 (5), 113–132.
Kishishita, T., Saito, E., Sagara, M., Fukui, J., Ooshita, T., 2003. Dynamic behavior of an existing foundation reinforced with micropiles. Doboku Gakkai Ronbunshuu 745 (I-65), 191–202 (in Japanese).
Nishioka, H., Koda, M., Tateyama, M., Kita, N., Hirao, J., Higuichi, S., 2008. A study on the characteristics of lateral resistance in footing foundation with sheet piles based on static loading tests. Doboku Gakkai Ronbunshuu C 64 (2), 383–402 (in Japanese).
Sugano, Y., Tamura, H., Eto, K., Kimura, M., Isobe, K., Nishiyama, Y., 2009. Overview of the program for steel pipe sheet pile foundations based on three-dimensional frame analysis and a design example using H-joint steel pile sheet piles. In: Proceedings of 44th JGS Annual Meeting, pp. 1227–1228 (in Japanese).
Ye, B., Ye, G., Zhang, F., Yashima, A., 2007. Experiment and numerical simulation of repeated liquefaction–consolidation of sand. Soils Found. 47 (3), 547–558.
Zhang, F., Kimura, M., Nakai, T., Hoshikawa, T., 2000. Mechanical behavior of pile foundations subjected to cyclic lateral loading up to the ultimate state. Soils Found. 40 (5), 1–17.
Zhang, F., Kimura, M., 2002. Numerical prediction of the dynamic behaviors of an RC group-pile foundation. Soils Found. 42 (3), 77–92.